TASK QUARTERLY 15 No 3–4, 297–315

SIMULATION OF RESIDENCE TIME DISTRIBUTION AND MIXING IN REACTORS WITH RECIRCULATION USING 2D APPROACH

PIOTR ZIMA

Faculty of Civil and Environmental Engineering,
Gdansk University of Technology,
Narutowicza 11/12, 80-233 Gdansk, Poland
pzim@pg.gda.pl

(Received 4 June 2011; revised manuscript received 2 September 2011)

Abstract: In this paper, we propose a 2D approach in order to create a mathematical model for the determination of the residence time distribution for a flow reactor with recirculation. Apart from characterizing the functional residence time distribution, this model can help improve the operation of the reactor at the design stage. The mathematical model was validated by comparison with experiments carried out in a hydraulic laboratory.

Keywords: mathematical modeling, residence time distribution, reactors with recirculation, 2D approach

1. Introduction

In the last few years, residence time distribution (RTD) has become an important tool for the analysis of industrial units and reactors, especially those used in waste-water treatment plants [1]. This problem is very often associated with determining functional characteristics of an object. By RTD characteristics of flow reactors we mean a set of parameters and state variables that contain complete information on the operation of a flow reactor. Here, two approaches are possible: the determination of these characteristics by a tracer study or numerical simulations using hydrodynamic models. Models obtained by tracer experiments are often restricted to the use of elementary reactors, such as perfect mixing cells in series or plug flow with axial dispersion [1]. The resulting information is often insufficient for the understanding of complex processes, where recirculation takes place. Until now, the determination of hydrodynamic behavior has mainly been limited to two extreme approaches. The first one is RTD analysis using simple

models, which produces general parameters, such as the number of mixing cells. The second one consists in using hydrodynamic models, which provide an accurate description of the flow pattern. The first method sometimes proves insufficient, whereas the second approach can be limited due to the complexity of the process under study [1].

In this paper, a 2D mathematical model for the determination of the RTD of a flow reactor with recirculation is proposed. The model is capable of producing functional RTD characteristics, however, it can also act as a supporting tool for improving the operation and design of a reactor at the design stage. This mathematical model was tested using data from physical experiments carried out in a hydraulic laboratory.

2. Model

The determination of functional characteristics of flow requires solving two fundamental problems: the determination of hydrodynamic behavior of a mixture, and the description of unsteady transport of the dissolved matter. The first problem concerns the description of the flow of a mixture of carrier fluid and solute through the reactor. This problem can be described by the Navier-Stokes equation (NSE). The NSE in the general form can be written as follows [2]:

$$\frac{D\boldsymbol{u}}{Dt} = \boldsymbol{f} - \frac{1}{\rho}\nabla p + \nu\Delta\boldsymbol{u} \tag{1}$$

together with the continuity equation:

$$\nabla\boldsymbol{u} = 0 \tag{2}$$

where $\boldsymbol{u}$ represents the velocity vector, $\boldsymbol{f}$ is the vector of external forces, p is pressure, ρ is density and ν is the kinematic viscosity factor. Equation (1) describes a three-dimensional time-dependent incompressible flow and, in practice, is very often supplemented (*cf.* turbulence models) and simplified depending on the flow conditions. In hydromechanics, there are many models which allow to describe the velocity field of flowing water [3], *e.g.* the kinematic model. This model assumes that the fluid particles undergo translational motion and rotation [4]. For the two-dimensional velocity vector:

$$\boldsymbol{u} = [u_x, u_y] \tag{3}$$

this condition can be written as follows:

$$\mathrm{rot}\,\boldsymbol{u} = \Omega(x,y) \tag{4}$$

where $\Omega(x,y)$ is an assumed function of vorticity distribution.

If we introduce the Stokes assumption (the omission of inertia forces) into the motion model (1) for the steady conditions of flow and a constant temperature of the mixture, and take into account relation (4), we obtain:

$$\Delta\Omega = 0 \tag{5}$$

This is the equation for a harmonic function of Ω, termed the Helmholtz equation. If we define a stream function $\psi(x,y)$ as follows [4]:

$$u_x = \frac{\partial \psi}{\partial y} \tag{6a}$$

$$u_y = -\frac{\partial \psi}{\partial x} \tag{6b}$$

we can finally write Equation (5) (the biharmonic equation) in the following form:

$$\Delta\Omega = \Delta\Delta\psi = \frac{\partial^4 \psi}{\partial x^4} + 2\frac{\partial^4 \psi}{\partial x^2 \partial y^2} + \frac{\partial^4 \psi}{\partial y^4} = 0 \tag{7}$$

Equation (7) can be interpreted as a generalization of kinematic models, in which the rotation of velocity is a harmonic function described by the Laplace equation. The application of the model (7) is known in the literature as the solution of the two-dimensional Stokes problem [5]. The omission of the impact of inertia forces in Equation (1) obviously influences the scope of such a model in its practical applications. If we assume that the operator Ω refers to a two-dimensional area bounded by an edge Γ and with the three functions f, g_1 and g_2, then in general we consider the Dirichlet problem for the biharmonic operator:

$$(P_0) = \left\{ \begin{array}{l} \Delta^2 \psi = f \\ \psi|_\Gamma = g_1 \\ \frac{\partial \psi}{\partial n} = g_2 \end{array} \right\} \tag{8}$$

The solution of problem (8) in two-dimensional space (x,y) is a stream function $\psi(x,y)$. Subsequently, using relations (6a) and (6b) we can calculate the components of the velocity vector $\boldsymbol{u}$ (4) in the entire domain.

The transport of the solute component i is described, in the most general form, by [6]:

$$\frac{Dc_i}{Dt} = \operatorname{div}\left[(D_i \boldsymbol{E} + \boldsymbol{D}_T)\operatorname{grad} c_i\right] + \sum_{j=1}^{n} S_{i,j} \tag{9}$$

where:

c_i – concentration of the component i (substance),
D_i – molecular diffusion coefficient,
$\boldsymbol{E}$ – unit tensor,
$\boldsymbol{D}_T$ – turbulent transport coefficient tensor:

$$[D_T] = \begin{bmatrix} D_{TL} & 0 & 0 \\ 0 & D_{TH} & 0 \\ 0 & 0 & D_{TV} \end{bmatrix} \tag{10}$$

where: D_{TL}, D_{TH}, D_{TV} – longitudinal, horizontal and vertical coordinates of the dispersion tensor,

$\sum_{j=1}^{n} S_{i,j}$ – sum of source functions (n), which describe the influence of the additional processes on the concentration c_i.

In the case of a flat two-dimensional domain, in which the velocity field is described by vector (3), the transport Equation (9) for an unreactive, permanent substance ($\Sigma S_{i,j} = 0$) can be written as follows [6, 7]:

$$\frac{\partial c_i}{\partial t} + \frac{\partial (u_x c_i)}{\partial x} + \frac{\partial (u_y c_i)}{\partial y} = \frac{\partial}{\partial x}\left(D_{xx}\frac{\partial c_i}{\partial x} + D_{xy}\frac{\partial c_i}{\partial y}\right) + \frac{\partial}{\partial y}\left(D_{yx}\frac{\partial c_i}{\partial x} + D_{yy}\frac{\partial c_i}{\partial y}\right) \tag{11}$$

where:

$$D_{xx} = D_L n_x^2 + D_H n_y^2 \tag{12a}$$

$$D_{xy} = D_{yx} = (D_L - D_H) n_x n_y \tag{12b}$$

$$D_{yy} = D_L n_y^2 + D_H n_x^2 \tag{12c}$$

The longitudinal and horizontal coordinates of the dispersion tensor (10) are described by the Elder formulas [8]:

$$D_L = 5.93 \cdot H v* \tag{13a}$$

$$D_H = 0.23 \cdot H v* \tag{13b}$$

$\boldsymbol{n}$ – directional velocity vector:

$$n_x = \frac{u_x}{|\boldsymbol{u}|} \tag{14a}$$

$$n_y = \frac{u_y}{|\boldsymbol{u}|} \tag{14b}$$

$v*$ – dynamic velocity [9]:

$$v* = \frac{n_M \sqrt{gu}}{R_h^{1/6}} \tag{15}$$

where:

n_M – the Manning coefficient,
g – acceleration due to gravity,
u – average velocity,
R_h – hydraulic radius.

In this paper, the values of the longitudinal dispersion coefficient D_L were estimated using optimization with a mean-square error test of convergence as the objective function. Subsequently, taking into account the Elder formula (13a), the Manning coefficient n_M (15) was determined and taken as the basis for the determination of the dispersion coefficient D_T (13b).

Equations (7) and (11) are partial differential equations, which, in general, are solved only by means of numerical methods, such as the finite difference method (FDM), the finite element method (FEM) and the finite volume method (FVM) [10, 11]. In this study, we use the FDM for the biharmonic equation [12] and the FVM for the unsteady transport equations [11]. In order to apply these

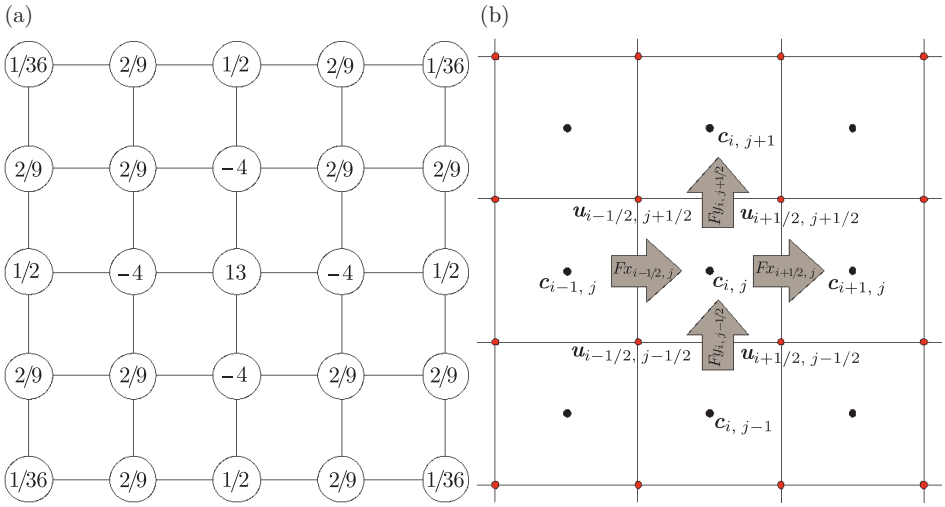

Figure 1. Decomposition of the domain into two-dimensional cells and the parameters of the models adopted in the solution of the biharmonic (a) and unsteady solute transport (b) equation

methods, we divided the domain into square elements (cells), with $\Delta x = \Delta y = h$ (*cf.* Figure 1), and n nodes in the x direction and m nodes in the y direction.

In the case of the biharmonic equation, as a result of the applied approximation of the difference quotients, an equation is obtained for each computational node. Figure 1, panel (a) shows the values of the coefficients at each node (i,j) resulting from adopting a central difference scheme (a modified 25-point scheme [12]) to approximate Equation (7). In the case of boundary nodes, the above scheme was modified according to the specified boundary condition, in accordance with (8). These equations are linear and form a system that can be solved with one of the known iterative methods. In this paper, the over-relaxation method was adopted [12]:

$$\psi_{i,j}^{(k+1)} = \psi_{i,j}^{(k)} + \frac{\omega}{4} r_{i,j}^{(k)} \tag{16}$$

where k indexes subsequent iterations, ω is the over-relaxation coefficient, $r_{i,j}$ is the residual of the approximation of the biharmonic equation at a given node. The final step is the calculation of the components of the velocity vector in the entire domain, in accordance with relations (6a) and (6b). The partial derivatives in Equations (6a) and (6b) were approximated by the corresponding central difference schemes.

When applied to the solution of the unsteady transport equation, the FVM refers to the physical conservation laws at the control volume level. This can be described by the homogeneous hyperbolic equation [11]:

$$\frac{\partial \boldsymbol{c}}{\partial t} + \nabla \cdot \boldsymbol{F} = 0 \tag{17}$$

Equation (11) can be written in vector form (17). In the case of the pure advection equation, the flux $\boldsymbol{F}$ in Equation (17) can be defined as:

$$\boldsymbol{F} = \boldsymbol{u} \cdot c \tag{18}$$

If during the flow of the solute we consider dispersion flux, which is described by an analog of the Fick's law [6], the flux $\boldsymbol{F}$ can be defined as follows [11]:

$$\boldsymbol{F} = \boldsymbol{u} \cdot c - D \cdot \nabla c \tag{19}$$

Integrating Equation (17) in each finite volume, and applying the Gauss-Ostrogradsky theorem, we obtain the following equation [11]:

$$\frac{\partial c_i}{\partial t} \Delta A_i + \oint\limits_{L_i} (\boldsymbol{F} \cdot \boldsymbol{n}) dL = 0 \tag{20}$$

where ΔA_i and L_i are, respectively, the surface area and the edge of the cell, and the flux $\boldsymbol{F}$ is defined by Equation (19). This integral represents the advection-dispersion mass flux of the substances through the edge of the cell. When rectangular elements are used, each integral in Equation (20) can be replaced by a sum over four components, as follows:

$$\frac{\partial c_i}{\partial t} \Delta A_i + \sum_{r=1}^{4} (\boldsymbol{F}_r \cdot \boldsymbol{n}_r) \Delta L_r = 0 \tag{21}$$

where $\boldsymbol{F}_\mathrm{r}$ is the vector of the streams through the edge r, and ΔL_r is the length of the edge of the cell. In this paper, we used a regular Cartesian square grid. This grid coincided with the differential grid used to solve the biharmonic equation (Figure 1, panel (b)). Therefore, the streams through the edge in Equation (21) will also coincide with the Cartesian x and y directions. The components of the flux vector through the edges x and y have the following form:

$$F_x = F_{Ax} + F_{Dx} = u_x \cdot c - D_{xx} \cdot \frac{\partial c}{\partial x} - D_{xy} \cdot \frac{\partial c}{\partial y} \tag{22}$$

$$F_y = F_{Ay} + F_{Dy} = u_y \cdot c - D_{yy} \cdot \frac{\partial c}{\partial y} - D_{xy} \cdot \frac{\partial c}{\partial x} \tag{23}$$

In order to solve Equation (11), a splitting technique was applied [11]. The transport of the dissolved matter was split into autonomous processes of advection and dispersion. In order to determine the numerical fluxes through the cell edge in the advection equation, the Lax-Wendroff scheme was used [11]. In the case of the dispersion equation, central difference schemes were used. In order to integrate Equations (22)–(23), we assumed that the control area is equivalent to the grid cell. In this approach, the values of the velocity vector $\boldsymbol{u}$ are given at the grid points and the functions located in the central points of the cells (Figure 1, panel (b)) are unknown. The determination of the intermediate values between the grid nodes (required to determine the value of the fluxes through individual cell edges) were calculated by averaging the neighboring values. This

approach was applied to the function of the concentration and the components of the velocity vector.

3. Laboratory experiment

In order to determine the basic parameters used in the model of solute transport (the tensor of dispersion, the Manning coefficient n_M) and to verify the adopted mathematical model, a tracer study was carried out in a hydraulics laboratory, using a model of a flow reactor with recirculation [13]. As a tracer, we used rhodamine WT (RWT) [14].

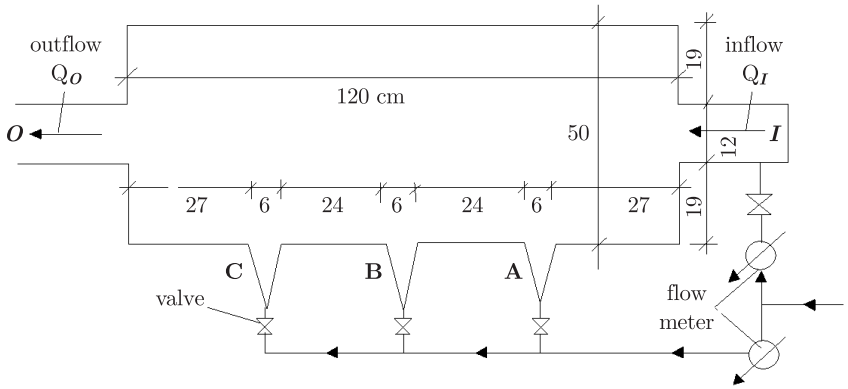

Figure 2. Schematic of the laboratory model

Laboratory tests were carried out in a rectangular tank made of stainless steel. Its shape and dimensions are shown in Figure 2. The position of the bottom allowed to create a layer of flowing water with a depth of about 3cm. In the tank, five holes were cut out in order to supply and drain water. Two of these were located along the bottom of the tank (to supply and return water from the mainstream): inlet ***I*** (inflow) and outlet ***O*** (outflow), and three of these were located below the bottom, on a side wall, to provide for the recirculation of water. The model was fed from a water supply system through a closed pipe system equipped with flow meters and valves. Two submersible probes (Cyclops-7, Turner's Design) were clamped for the continuous measurement of the RWT concentration at four different points (R_1–R_4) along with a propeller for the continuous measurement of velocity at four points (M_1–M_4) (see Figure 3).

For the purposes of this study, a custom fixed-dose tracer dispensing system was built. This system allowed to carry out fully repeatable experiments. The details of the performed laboratory tests are presented in [13].

During a comprehensive study of the reactor in the laboratory, we carried out tests, which allowed us to investigate the distribution of the tracer in the reactor, depending on different variants of water supply and recirculation. To the longitudinal flow (inlet of the stream at ***I***, outlet at ***O***) we added a side stream (corresponding to a one-turn recirculation) from one of the inlet sides:

A, ***B*** or ***C***. During the experiments steady flow conditions were assumed. The following degrees of recirculation were simulated (the ratio of the flow at the inlet of the tank Q_I and to the side inlet flow Q_x [$x = A$, B or C]) – $Q_I : Q_x$: 6 : 1, 3 : 1, 2 : 1, 1 : 1, 1 : 2, 1 : 3 and 1 : 6. The total flow ($Q_I + Q_x$) was always equal to 0.8dm^3/s. The Manning coefficient n_M was determined experimentally. This allowed us to calculate the components of the dispersion tensor. The parameters from Equation (27) were also determined during optimization. Equation (27) was used for the simulation of the tracer injection at points ***A***, ***B*** and ***C***.

4. Numerical calculations and discussion

Numerical simulations were performed according to the laboratory measurements. These simulations allowed us to calculate the velocity field and the distribution of RWT concentration in the analyzed model of the reactor. The simulations were performed for all variants of laboratory tests. For this purpose, the continuous reactor domain was discretized using a square grid with a step of $\Delta x = \Delta y = 1$cm, where in the x direction there were $n = 181$ nodes and in the y direction we had $m = 51$ nodes. The numerical simulations were carried out under steady conditions of water flow and unsteady conditions of the solute transport.

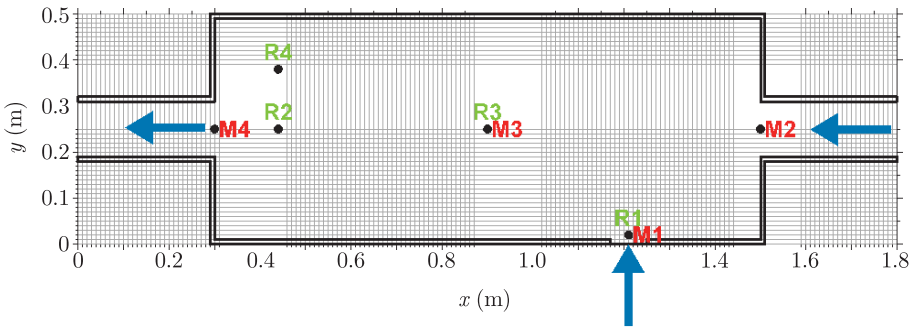

Figure 3. Numerical domain with a grid and the distribution of measurement probes for the inlet of recirculation (type A)

For the calculation of the velocity field under steady conditions, we applied the kinematic model (7). Equation (7) is an elliptic differential equation of the fourth order, the solution of which requires two conditions:

- a Dirichlet condition – a known value of the stream function, where $\psi = \text{const.}$ at the impervious boundary and $\psi = \text{varians}$ at the pervious boundary;
- a Neumann condition at the impervious boundary:

$$\frac{\partial \psi}{\partial n} = 0 \tag{24}$$

Example results (the distribution of stream lines and velocity vectors) for the water supply by inlet ***I*** and side inlet ***A*** are shown in Figure 4, panel (a) – for the ratio of $Q_I : Q_A = 1 : 3$, and in Figure 4, panel (b) – for the ratio of

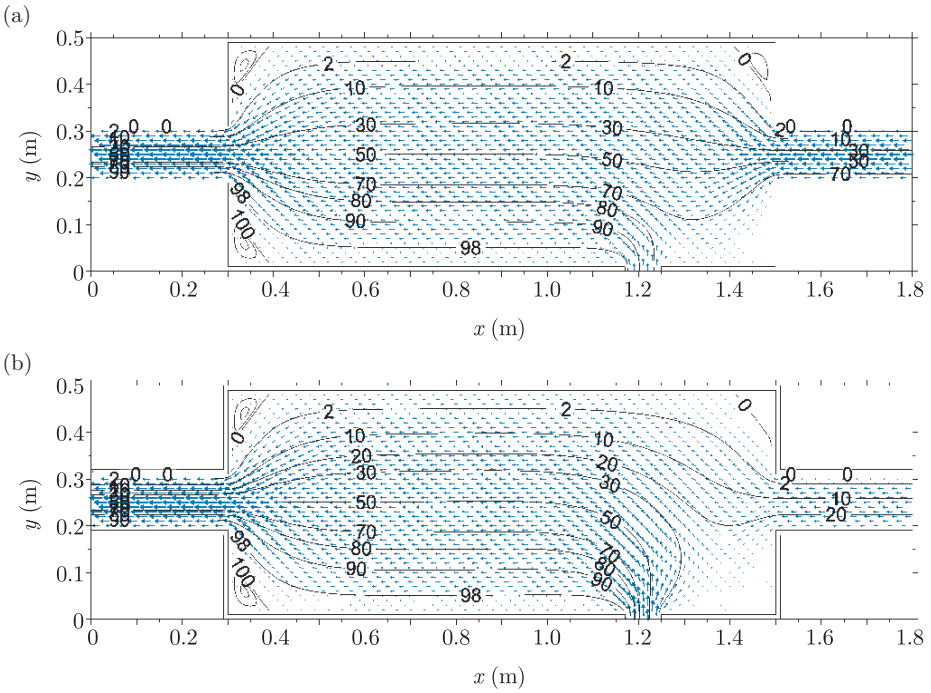

Figure 4. The distribution of the stream function and velocity field: (a) $Q_I : Q_A = 1:3$, (b) $Q_I : Q_A = 3:1$

$Q_I : Q_A = 3:1$. In the figures, the stream lines are scaled-down – 100% corresponds to the maximum flow rate of $0.8\,\mathrm{dm}^3/\mathrm{s}$. Velocity vectors were determined using (6) and were scaled relative to the maximum speed of $0.25\,\mathrm{m/s}$. These results were verified during velocity measurements. Subsequently, we simulated transient tracer transport. The solution of Equation (11) was superimposed onto the calculated velocity field. Equation (11) is a partial differential equation of the second order whose solution requires the following boundary conditions:

- an initial condition – the tracer concentration $c(x,y)$ at the initial time (in this case, $c = 0.0\,\mathrm{ppb}$);
- a boundary condition on the impermeable edge of the domain (a Neumann condition):

$$\frac{\partial c}{\partial n} = 0 \tag{25}$$

- a boundary condition on the permeable edge of the domain (a Dirichlet condition):

$$c = \mathrm{const.} \tag{26}$$

At the point of tracer input with recirculation, the concentration of the tracer was determined from a one-dimensional analytical solution of the unsteady advection-diffusion equation of the following form [15]:

$$C(x,t) = \frac{M}{2\sqrt{D_L \pi t}} \exp\left[-\frac{(x - x_0 - ut)^2}{4 D_L t}\right] \tag{27}$$

u – mean velocity,
x_0 – position of the impulse with an intensity M,
M – impulse intensity:

$$M = M_0 \cdot \delta(x - x_0) \tag{28}$$

δ – the Dirac delta function

$$\delta = \begin{cases} +\infty, & x = x_0 \\ 0 & x \neq x_0 \end{cases} \tag{29}$$

The delta function has the following property:

$$\int_{-\infty}^{+\infty} \delta(x - x_0)dx = 1 \tag{30}$$

For the permeable domain (outlet boundary), a simplified boundary condition based on the omission of diffusive flux was used [16].

Example results (the distribution of tracer concentration after the simulation was terminated) for two chosen cases are shown in Figure 5 – for the ratio of $Q_I : Q_B = 3:1$, and in Figure 7 – for the ratio of $Q_I : Q_B = 1:3$.

5. Mathematical model of the reactor

One of the components of the concentration curve in the final cross-section of the reactor can constitute an example of an RTD characteristics. This curve can be determined experimentally (during the tracer study) or theoretically, based on the developed mathematical model of the reactor.

In the case of experimental determination of the RTD characteristics (Figures 6 and 8), the concentration curve can reflect only the behavior of the unreactive permanent substance (tracer). However, to create the full characteristics of the object, it may be necessary to include the source processes S in Equation (11). This function presents the retention time of individual parts of the tracer doses brought into the inlet cross-section, and is identical with the RTD curve [13]. The examples of the characteristics observed in the laboratory tests are shown in Figure 9. These characteristics describe the distribution of the unreactive, permanent substance in response to an impulse (27) injected through the inlet $\boldsymbol{A}$.

The mathematical model of the reactor enables the theoretical determination of the RTD characteristics of an object, as well as a practically unlimited analysis and simulation of the processes taking place in the reactors [1, 17]. This analysis extends beyond the research capabilities of the experiments performed in the laboratory and could also affect the flow through the reactor of two different, permanent substances or substances subject to a specific source processes.

The implementation of concentration measurements of the flow of various substances (two or more) through the reactor, even under laboratory conditions, may pose certain technical problems. For instance, it can be difficult to find

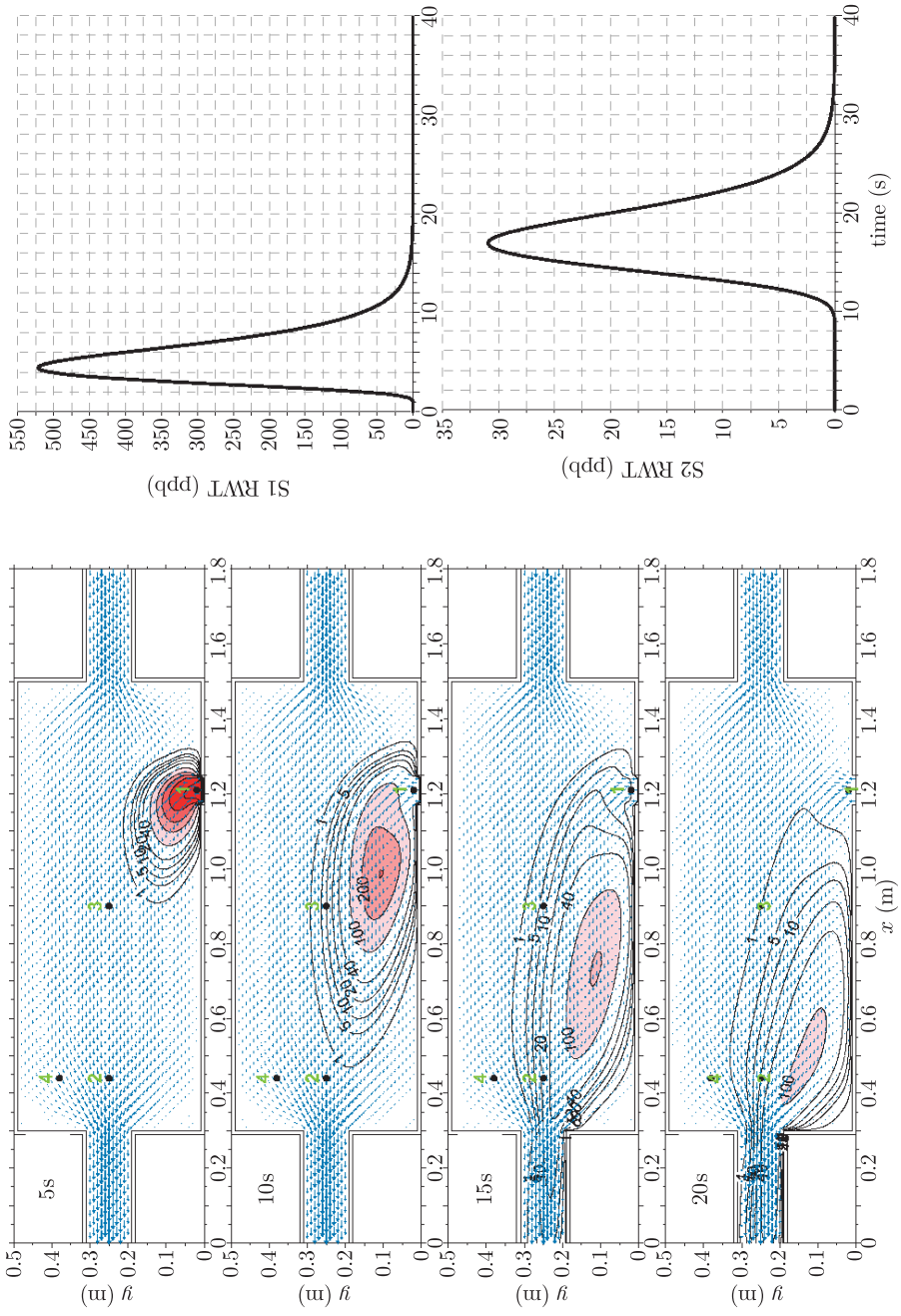

Figure 5. Distribution of tracer concentration over time for the supply (variant A), where $Q_I : Q_A = 3:1$

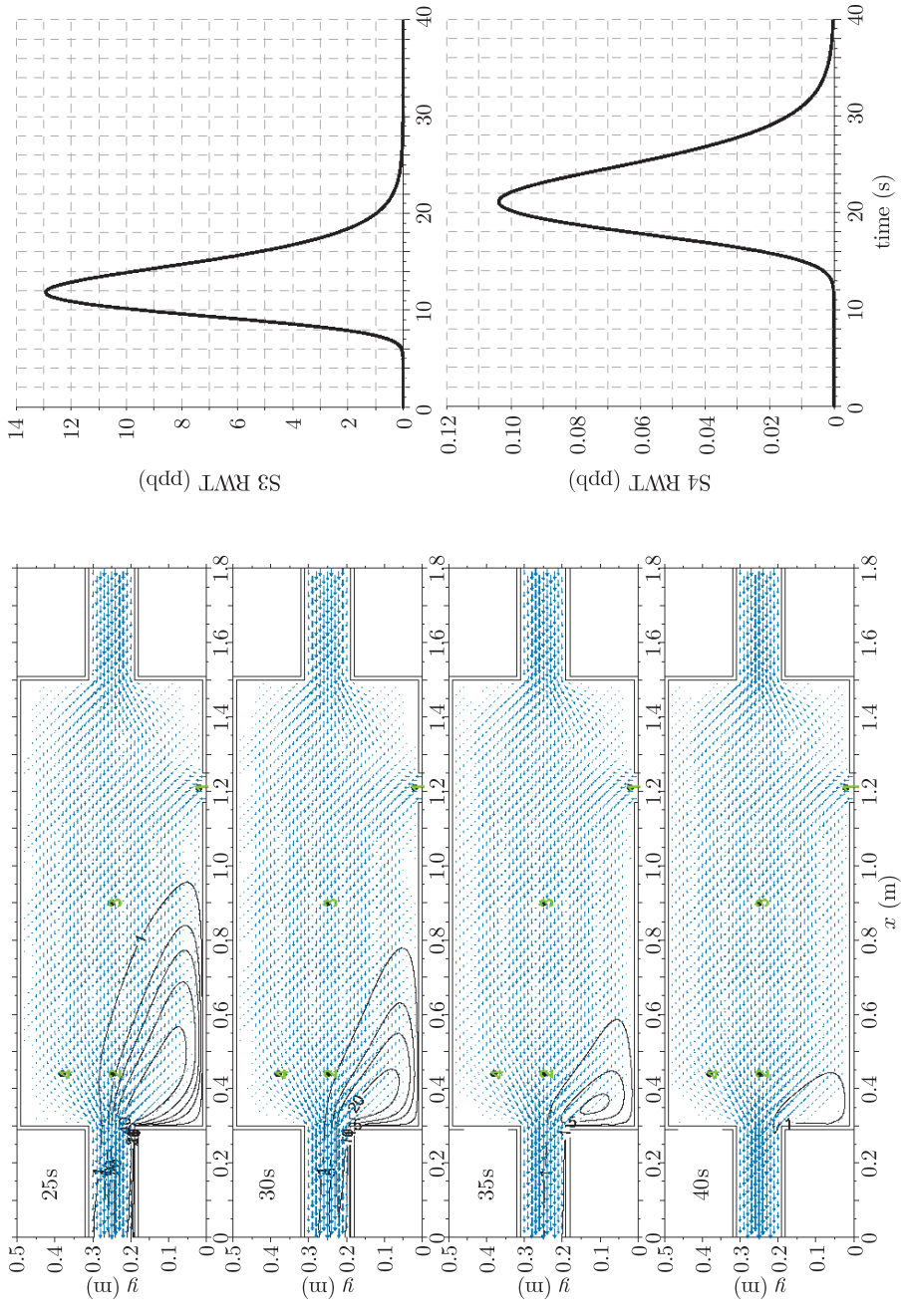

Figure 5 – continued. Distribution of tracer concentration over time for the supply (variant A), where $Q_I : Q_A = 3 : 1$

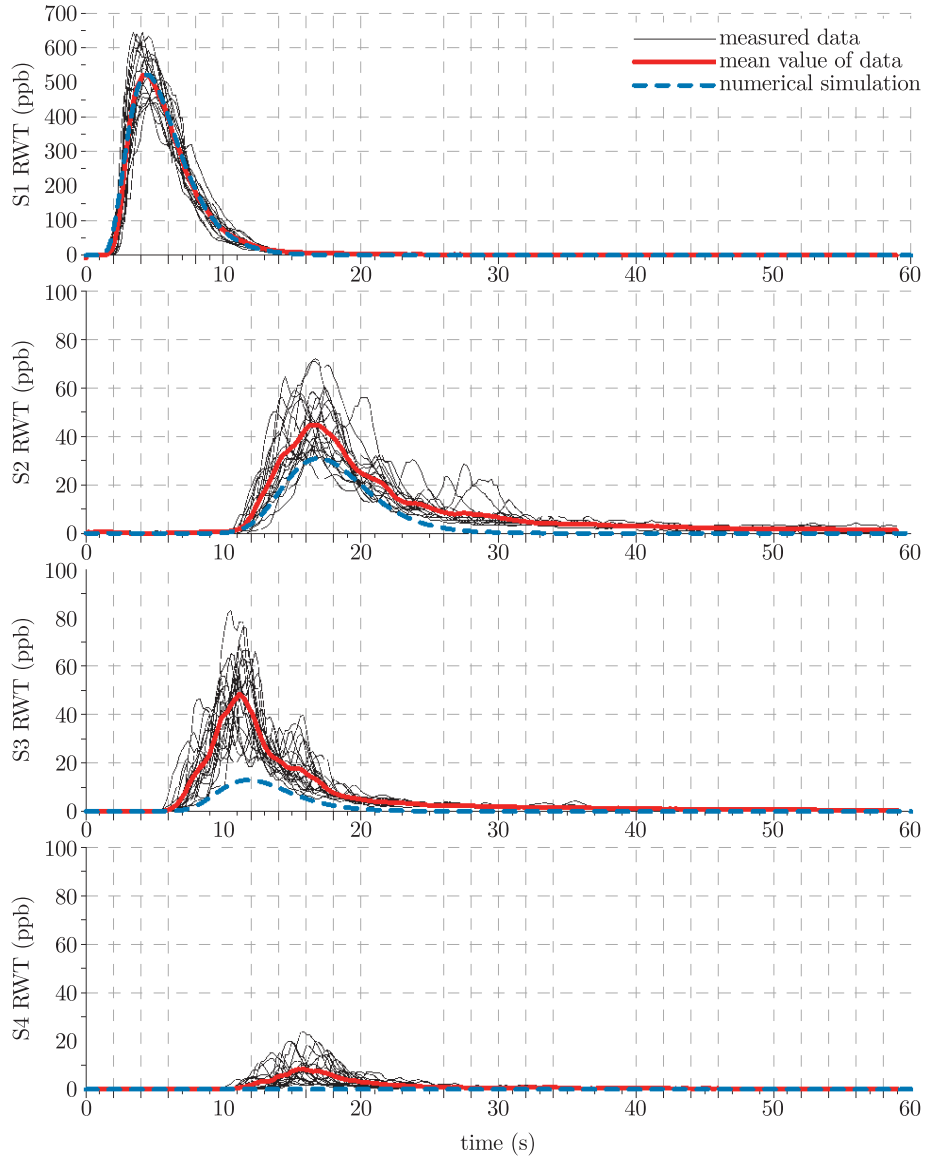

Figure 6. Results of the measurements of RWT concentration and the numerical simulation for variant A, where $Q_I : Q_B = 3 : 1$

measuring instruments operating selectively on certain substances (especially in the case of fluorometric measurements, and other [18]). The solution of this problem through mathematical modeling, on the other hand, should pose no major problems. The simulation results of flow through the reactor for two doses of a substance injected through various inlets (***I*** and ***A***) are shown in Figure 10. The results of these simulations can help determine the RTD characteristics for this case.

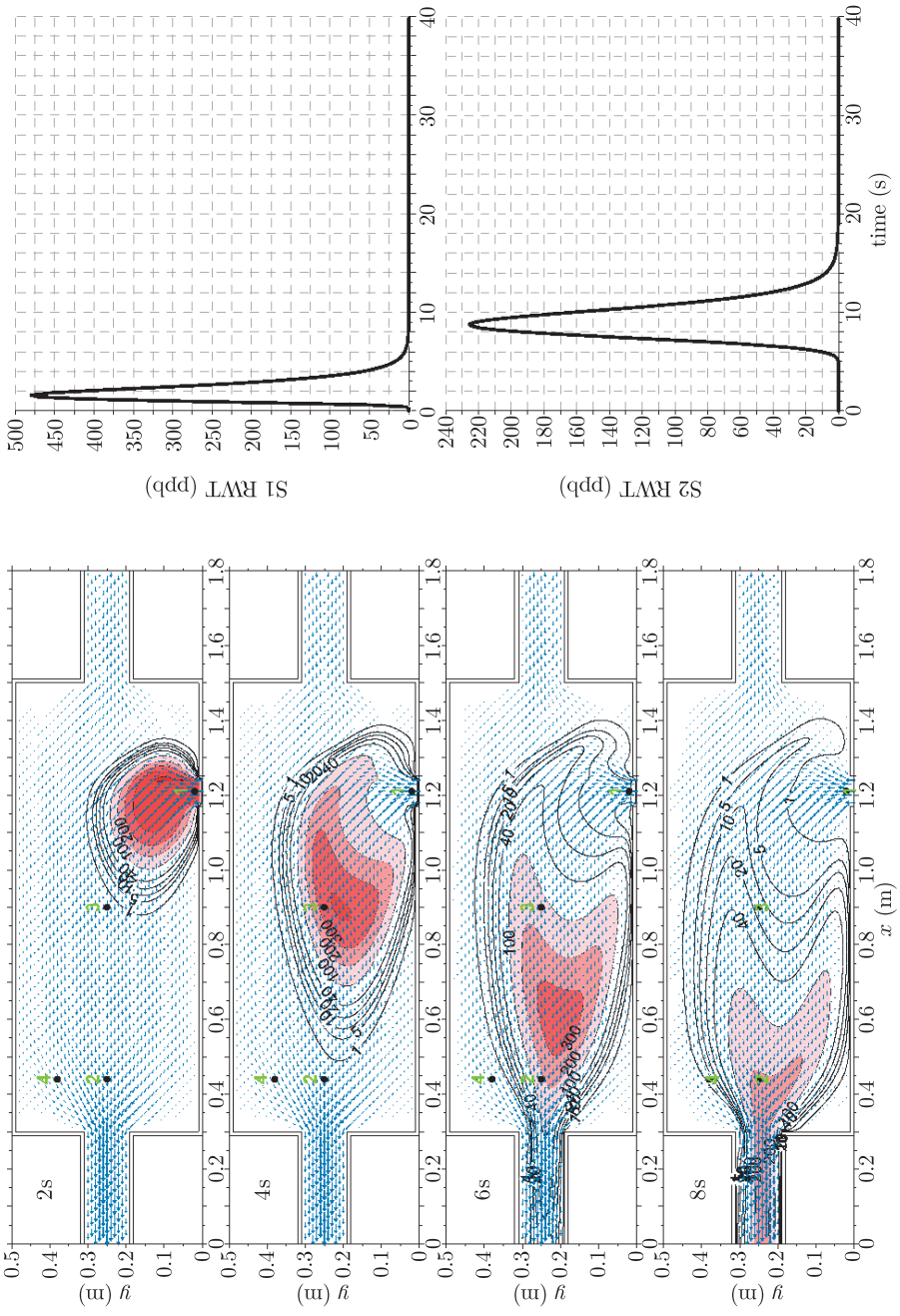

Figure 7. Distribution of tracer concentration over time for the supply (variant A), where $Q_I : Q_B = 1:3$

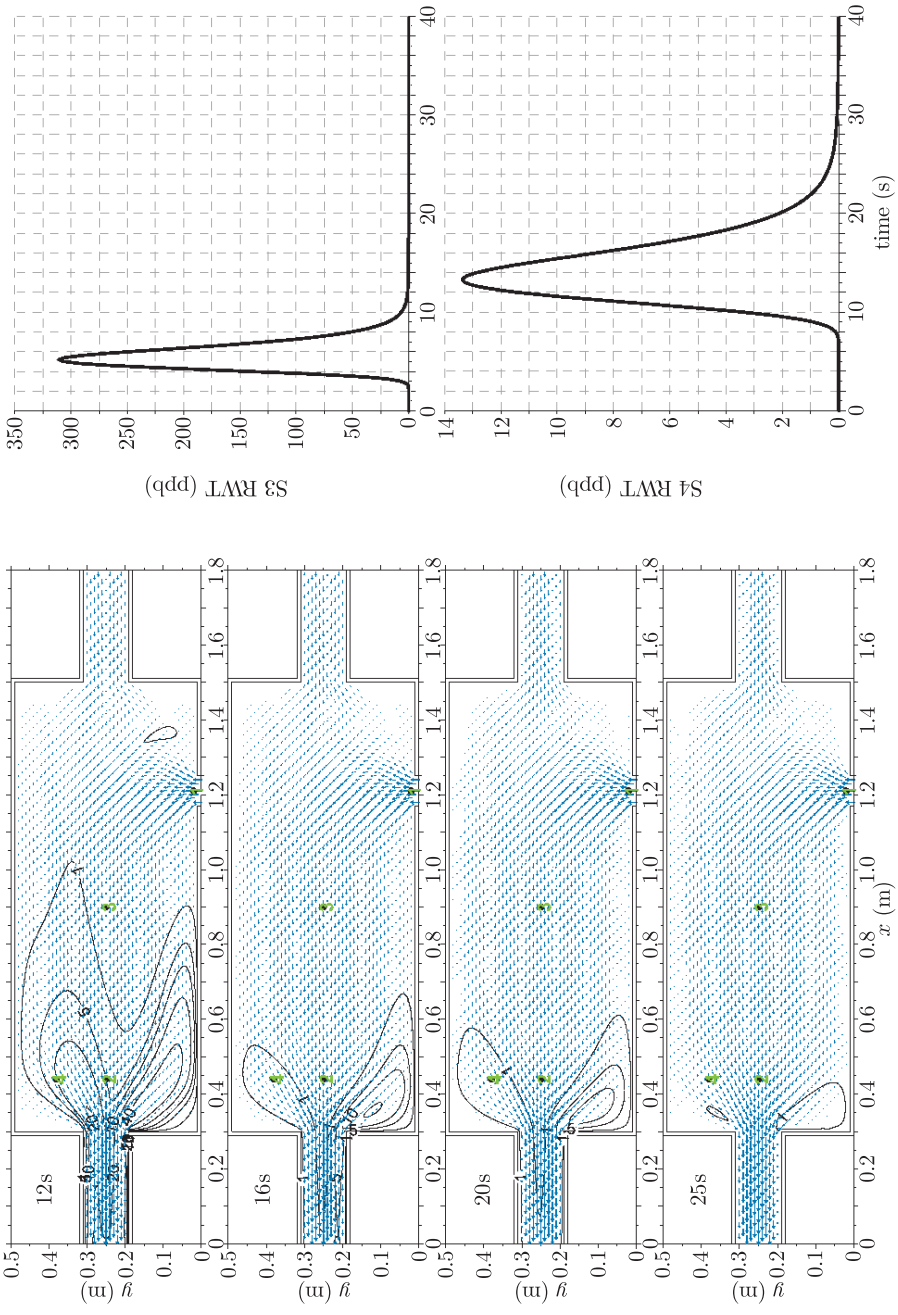

Figure 7 – continued. Distribution of tracer concentration over time for the supply (variant A), where $Q_I : Q_B = 1:3$

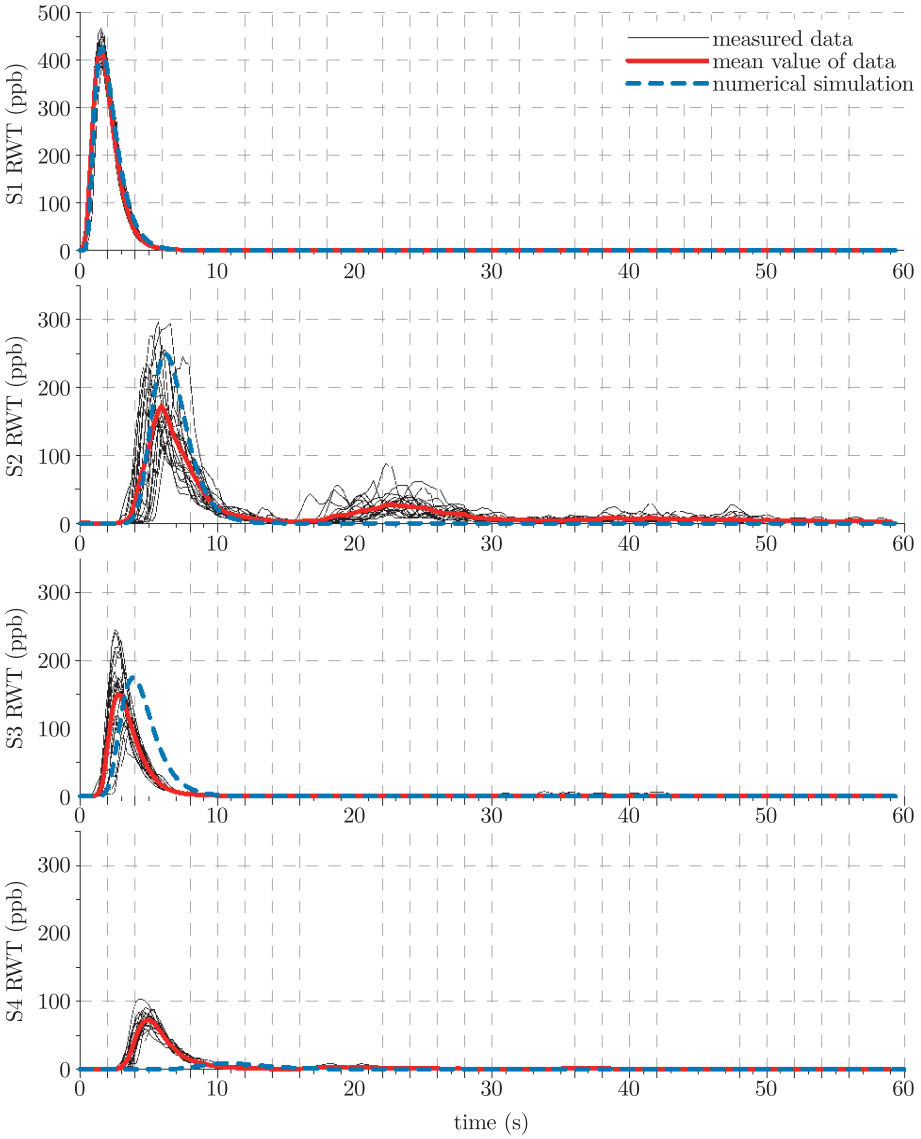

Figure 8. Results of the measurements of RWT concentration and the numerical simulation for variant A, where $Q_I : Q_B = 1:3$

Figure 11 presents the simulation results for the injection of substances (different substances which are permanent and passive) into the reactor, simultaneously through two different inlets (***I*** and ***A***). We can also consider the flow of substances which can react on contact with each other. This requires augmenting Equation (11) with a suitable definition of the functions describing these changes in the form of suitable source terms S. This information can be obtained on the basis of known formulas for the stoichiometry and kinetics of various chemical or biochemical reactions.

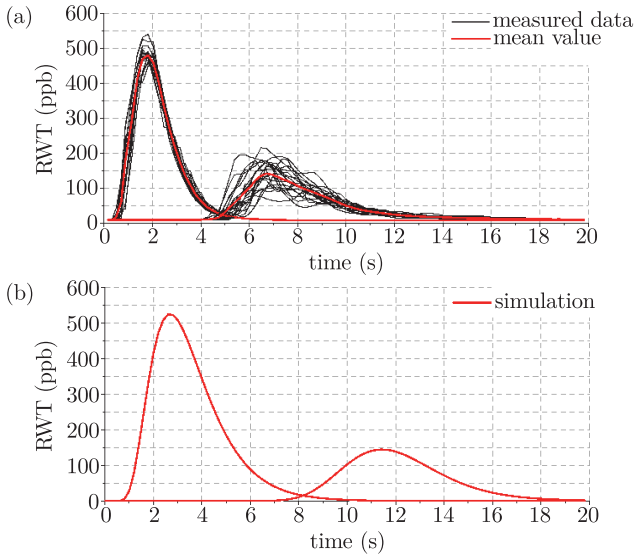

Figure 9. Examples of functional characteristics of the reactor (a) result of the tracer study carried out in a laboratory, (b) result of the numerical simulation

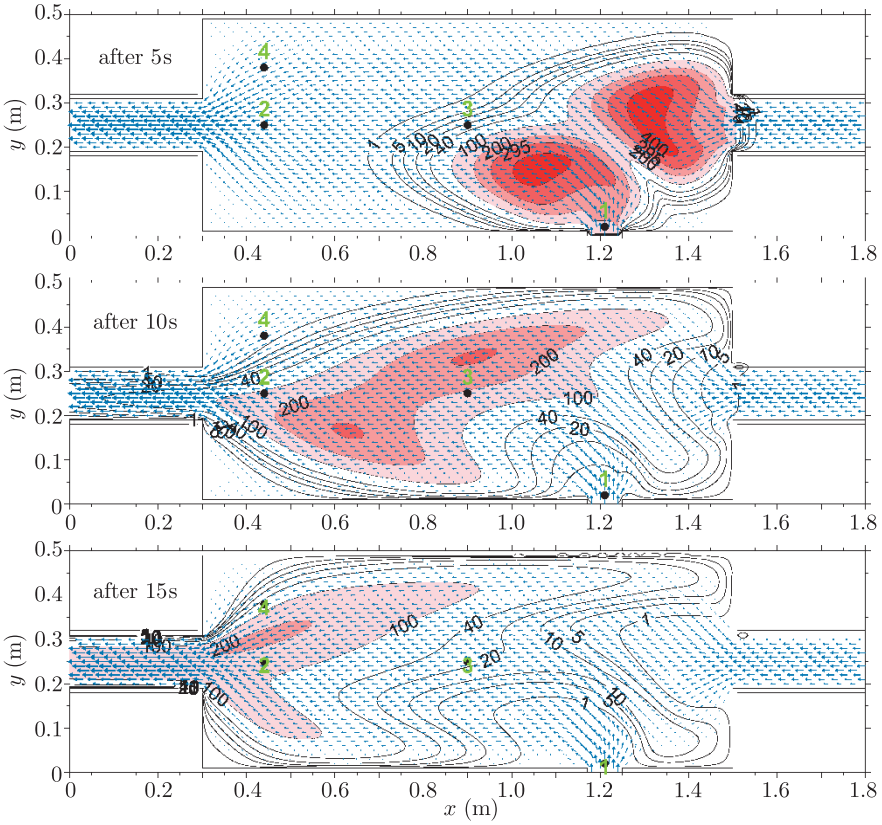

Figure 10. Simulation results for the injection of a substance (tracer) into the reactor, simultaneously through two inlets (***I*** and ***A***), and the results of their mixing

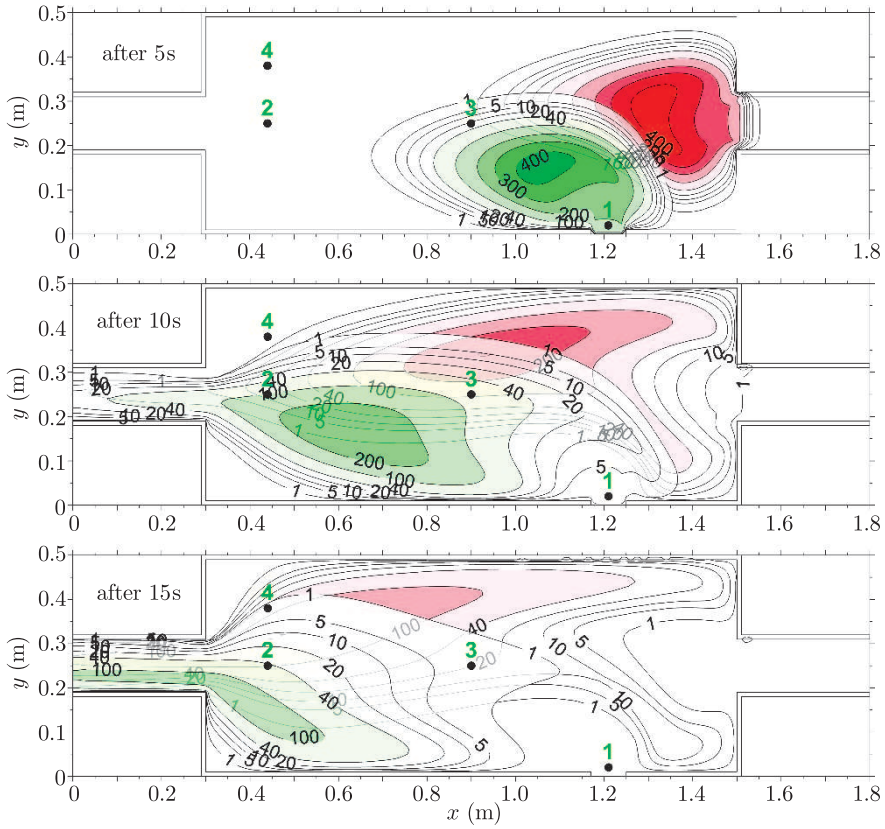

Figure 11. Simulation results for the injection of two different immiscible substances (tracers) into the reactor, simultaneously through two inlets (***I*** and ***A***)

6. Conclusions

The presented results of numerical simulations validated by comparing with laboratory measurements portend well for the possibility of creating a mathematical model of a reactor with recirculation flow. Therefore, it is important to include physical methods (supported by conservation equations) in the methodology on dimensioning objects and processes related to water and sewage purification [19, 20]. Compared with the common design guidelines in the form of simple algebraic dependencies, these methods are mathematically more complex (the more accurate the method, the more complex the equations). The creation of a mathematical model enables accurate analysis of the operated object at the design stage. This could result in models based on the solutions of the equations of mathematical physics [1, 17]. On the other hand, it would be unreasonable to expect that at the engineering (or operator) level, methods which require extensive knowledge of the solution (very often numerical) of the relevant equations describing the conservation laws will be used. Therefore, such a mathematical model could be applied, for instance, in order to determine the RTD characteristics of flow reactors [13].

Acknowledgements

The calculations presented in this paper were carried out at the TASK Academic Computer Center in Gdansk, Poland.

References

[1] Leclerc J, Claudel S, Lintz H, Potier O and Antoine B 2000 *Oil & Gas Science and Technology* **55** (2) 159
[2] Sawicki J M 1998 *Free Surface Flows*, PWN, Warsaw (in Polish)
[3] Anderson J D 1995 *Computational Fluid Dynamics*, McGraw-Hill Inc., New York
[4] Sawicki J M 2009 *Mechanics of Flows*, Gdansk University of Technology Press, Gdansk (in Polish)
[5] Glowinski R and Pironneau O 1977 *Raport STAN-CS-77-615*, Computer Science Department, School of Humanities and Sciences, Stanford University
[6] Sawicki J M 2003 *Migration of Pollutants*, Gdansk University of Technology Press, Gdansk (in Polish)
[7] Rutherford J C 1994 *River Mixing*, Wiley, Chichester, England
[8] Elder J W 1959 *J. Fluid Mech.* **5** (4) 544
[9] Taylor G J 1954 *Proc. Roy. Soc.* **223**–**224** 446
[10] Fletcher C A J 1991 *Computational Techniques for Fluid Dynamics 1. Fundamental and General Techniques*, Springer-Verlag, Berlin
[11] LeVeque R J 2002 *Finite Volume Method for Hyperbolic Problems*, Cambridge University Press, New York
[12] Kosma Z 2009 *Numerical Methods and Algorithms*, Technical University of Radom Press, Radom (in Polish)
[13] Sawicki J M, Malus D and Zima P 2008 *Hydraulics of Reactor with Recirculation*, Gdansk University of Technology Press, Gdansk (in Polish)
[14] Wilson J F, Cobb E D and Kilpatrick F A 1986 *U.S. Geological Survey Techniques of Water Resources Investigations* **3** (A12) 34
[15] Crank J 1975 *The Mathematics of Diffusion*, Clarendon Press, Oxford
[16] Zima P 2002 *Arch. Hydro-Eng. Environm. Mech.* **49** (2) 71
[17] Ekambara K and Joshi J B 2003 *Can. J. Chem. Eng.* **81** 669
[18] International Atomic Energy Agency 2008 *Radiotracer Residence Time Distribution Method for Industrial and Environmental Applications*, Training Course Series, Vienna, **31**
[19] Olivet D, Valls J, Gordillo M A, Freixó A and Sanchez A 2005 *J. Chem. Technol. Biotechnol.* **80** 425
[20] Sawicki J M 2009 *A Quantitative Description of the Issues of Environmental Engineering – Theory and Practice*, Lublin University of Technology Press, Lublin, **1** 269 (in Polish)